Surf. Sci., Subm. Feb. 2000

Ultrathin aluminum oxide films: Al-sublattice structure and the effect of substrate on ad-metal adhesion

D. R. Jennison* and A. Bogicevic**
Surface and Interface Sciences Department
Sandia National Laboratories, Albuquerque, NM 87185-1421 USA

Abstract

First principles density-functional slab calculations are used to study 5 Å (two O-layer) Al_2O_3 films on Ru(0001) and Al(111). Using larger unit cells than in a recent study, it is found that the lowest energy stable film has an even mix of tetrahedral (*t*) and octahedral (*o*) site Al ions, and thus most closely resembles the κ-phase of bulk alumina. Here, alternating zig-zag rows of *t* and *o* occur within the surface plane, resulting in a greater average lateral separation of the Al-ions than with pure *t* or *o*. A second structure with an even mix of *t* and *o* has also been found, consisting of alternating stripes. These patterns mix easily, can exist in three equivalent directions on basal substrates, and can also be displaced laterally, suggesting a mechanism for a loss of long-range order in the Al-sublattice. While the latter would cause the film to appear amorphous in diffraction experiments, local coordination and film density are little affected. On a film supported by rigid Ru(0001), overlayers of Cu, Pd, and Pt bind similarly as on bulk truncated α-Al_2O_3(0001). However, when the film is supported by soft Al(111), the adhesion of Cu, Pd, and Pt metal overlayers is significantly increased: Oxide-surface Al atoms rise so only they contact the overlayer, while substrate Al metal atoms migrate into the oxide film. Thus the binding energy of metal overlayers is strongly substrate dependent, and our numbers for the above Pd-overlayer systems bracket a recent experimentally derived value for a film on NiAl(110).

Keywords: Density functional calculations, Insulating films, Surface structure, Aluminum oxide, Metal-insulator interfaces, Chemisorption, Cu, Pd, Pt, Amorphous surfaces.

*Corresponding author: drjenni@sandia.gov
**Present address: Ford Research Company, Dearborn, MI 48121-2053

DISCLAIMER

Aluminum oxide films are of substantial current interest. First, they are relevant to the initial oxidation of Al metal and the 5-10 Å "barrier layer" which inhibits corrosion [1]. Second, they enable surface spectroscopic studies without charging or impurity problems, which often occur with bulk-truncated alumina [2, 3]. Third, when metal is deposited, the films model supported catalysts [4]. Finally, ultrathin Al_2O_3 films are used in microelectronics as dielectric, diffusion, and tunneling junction barriers [5]. However, in spite of considerable recent work, the film structure is poorly understood on an atomic scale, thus preventing a complete understanding of basic issues such as metal island nucleation [6], adhesion, and adatom diffusion (as explicitly seen in recent FIM experiments [7]).

Two O-layer 5 Å films are self-limited in thickness when made by NiAl [8] or Ni_3Al [9] oxidation. Here the films grow in a rotated domain structure (whose complexity prevents direct computations on these systems) and no Ni is present in the film [8-10]. HREELS evidence from Al_2O_3/NiAl(110) [10] suggests Al ions occupy a mixture of octahedral (*o*) and tetrahedral (*t*) sites in close-packed oxygen layers, which has led to these films being called "γ-like". More recently, TEM Moire patterns [11] have indeed indicated the film O-O spacing to be consistent with the γ-phase, but this result also allows other possible structures. Furthermore, the film thinness, at two O-layers, prevents a definable stacking, such as hcp or fcc which differentiates the α- and γ-phases. In fact, the structure of the Al-sublattice is unknown. However, an important clue has arisen from new experiments in the group of Behm [12], using Al deposition and oxidation on Ru(0001). This refractory substrate permits heating to significant temperatures and, while islands of 5Å Al_2O_3 can be seen at various coverages with STM, at high coverages LEED evidence rules out all Al ions occupying the same type of site. Furthermore, no or only weak ordering of the Al sublattice is found, in spite of annealing to over 900K.

On the theoretical side, lately a significant demonstration has appeared showing the reliability of density functional theory (DFT). A complex oxide phase, κ-Al_2O_3, was structurally analyzed completely by computation, and the predicted X-ray scattering pattern is in close agreement with experiments on CVD-grown samples [13]. In addition, DFT was recently used to study the unusual

distortions produced by a rare earth impurity in bulk α-Al_2O_3 (sapphire) [14]; the deep surface relaxations associated with sapphire (0001), and metal adsorption thereon [15]; and the nature of the interface between aluminum oxide ultrathin films and substrate metals [16]. A comprehensive survey of metal adsorption was also made using a model film structure [17].

Calculations of two and three O-layer Al_2O_3 films on Al(111), Mo(110) and Ru(0001) [16] produced three significant findings for these substrates: 1) the interface between the oxide film and the substrate is 1 ML of chemisorbed oxygen, 2) on top of which is a nearly coplanar layer of Al and O ions, 3) where the normal bulk preference for octahedral- (*o*) over tetrahedral-site (*t*) aluminum ions is energetically reversed. The latter result is caused by the electrostatics and layer separations induced by the interface with the underlying metal [16]. However, this initial work used only small unit cells (see Fig. 1), and did not allow the possibility of more complex structures. For films grown on the Ni-Al materials, the domain rotation presumably occurs between the first metallic Al layer (just below the second—i.e., chemisorbed—oxygen layer) and the substrate lattice, rather than between chemisorbed oxygen and the top metallic layer. (This, of course, would cost considerably more energy.)

In this paper, we report DFT [18] computational results on two O-layer alumina film morphology with both Ru(0001) and Al(111) substrates, obtained by expanding the unit cell and allowing a variety of *t*/*o* ratios and structures. Furthermore, we report a likely mechanism for the loss of long range order in the Al-sublattice, and a significant dependence of ad-metal adhesion on the nature of the supporting substrate. Note that these substrates differ considerably in stiffness and in cohesive energy.

Our electronic structure calculations were performed using the Vienna *Ab initio* Simulation Package (VASP) [19]. This plane-wave based density-functional code allows the use of Vanderbilt ultra-soft pseudopotentials [20], which provide good convergence for these systems with a plane wave cutoff of only 270 eV. We used both the standard local density approximation (LDA) [21] and the "PW91" generalized gradient approximation (GGA) [22]. Complete geometric relaxation was time consuming due to the mixture of hard and soft vibrational modes. A workable scheme was

found by first using a quasi-Newton algorithm, followed by final refinement with a damped dynamics scheme, both built into VASP. All relaxed structures had residual computed interatomic forces under 0.05 eV/Å. Our slab calculations consisted of Ru or Al metal layers with the oxide films on one face. The bottom metal layers (see below) were frozen at the bulk LDA or GGA (as appropriate) Ru or Al geometry, while all other atoms were free to relax. The vacuum gap between periodic slabs in the vertical direction was >18 Å, due to the magnitude of long range electrostatic forces.

We begin by utilizing the fundamental conclusions of Ref. [16]: First, chemisorbed 1x1 oxygen marks the film/substrate interface, which is bound strongly to the metal [5 eV/atom for Al(111)]. Next, we create an overlying layer of nearly coplanar Al and O ions, which thus achieve near layer neutrality, in spite of the surface appearing "oxygen terminated" in ISS experiments [10]. In order to consider only the lowest-lying energetic possibilities, we impose three constraints: 1) We do not allow non-stoichiometry in the film Al/O ratio; 2) We restrict coordination to what is normal (i.e., each surface O has two nearly coplanar Al nearest neighbors, Fig. 1); and 3) We do not consider geometries where *t* and *o* ions are immediately next to each other (i.e., at adjacent tetrahedral and octahedral sites, configurations much higher in energy due to Al-Al ionic repulsion).

Our analysis indicates that within the above constraints it is not possible to produce a localized *o*-containing "defect" starting with all *t*-ions, or visa versa. However, it is possible to produce a zigzag row of *o*-ions embedded in an otherwise perfect film of 100% *t*-ions by displacing a row laterally in the $[1\bar{2}0]$ direction of the basal plane of the underlying metal—downwards in Fig. 2—so as to move all the ions in that row from *t* to neighboring *o* sites. Note that the effect of this shift is to increase the average lateral Al-Al interatomic spacing (Fig. 2), and the latter is maximized if *t* and *o* rows alternate. With this arrangement, the resulting structure has a 2x1 unit cell (Fig. 2, right side) relative to the primitive cell of three O- and two Al-ions in the surface plane of the film, and an even (1:1) mixture of *t* and *o* Al ions.

It is already known that DFT is very accurate to determine aluminum oxide structures and relative energies [13, 15]. Since, however, our study necessitated numerous computations using large supercells, the following tests were performed to ensure accuracy: 1) The relative LDA energies of 2x1

supercells with all *o*, all *t*, and the zig-zag 1:1 mixture of Al rows were computed with seven layers of Ru substrate (bottom four frozen) and using eight k-points. Errors produced in *relative* energy by reducing the Ru slab to just four layers (bottom two frozen), and/or the number of k-points to two, were found to be < 0.1 eV, out of energy differences of ~ 2 eV per 2x1 cell. 2) Because numerical noise (arising from small inaccuracies in force computation) grow significantly during prolonged geometric relaxation, tests were done to examine the effect of freezing the entire Ru metal substrate (as mentioned above, these systems are very problematic because they mix hard and soft vibrational modes; all first-guesses had ions at the ideal positions with respect to the extended metal lattice). It was again found that errors were small, here below 0.05 eV per 2x1 cell. These results indicate that the relative energies, at least with the Ru substrate, are determined almost entirely by the electrostatics within the oxide film itself, which, because the bands are relatively flat, can be adequately described by few k-points.

In Table 1, we see the zig-zag 2:1 structure favored over either of the pure structures for both Ru and Al substrates. The energetic differences are so great that it is clear that the electrostatic advantage of maximizing the Al-Al lateral ion spacing dominates the *t* site preference reported in Ref. [16]. In Table 2, we see the vertical geometry of the structure compared with that of having all *t*-ions (cf. Fig. 1). Note that the film surfaces still consist of nearly coplanar Al- and O-ions, but that a surface buckling now exists with both substrates. This is caused by the reduced symmetry in the coordination of the surface O-sublattice with Al-ions (see Fig. 2). The buckling penetrates several layers into the Al metal and shows 1/3 of the surface metal has moved substantially upward, even *into* the first layer of oxygens. This does not happen in the case of the stiffer Ru substrate, whose cohesive energy is about twice that of Al.

It is now obvious that in principle one may have any mix of the two types of rows. For example, a 3:1 mixture of ion types would have a 4x1 cell (e.g., *-t-t-t-o-*), but a 2:1 ratio would result in a 6x1 cell because of a phase reversal of the zig-zag after a single *-t-t-o-* sequence. Note though, that these other arrangements all decrease the average lateral Al-Al ion separation compared with the 2x1 structure, and, since the lateral interaction dominates, these structures are not favored. Indeed, test

computations failed to find relaxed metastable geometries for the 2:1 and 3:1 ratios as, after many geometric steps, three-O-layer-thick stripes resulted which were separated by depleted regions, even when using very small steps. We take these results as further evidence that these hypothetical structures are higher in energy.

Interestingly, a second type of stable *-t-o-t-o-* 1:1 structure has also been found, consisting of alternating stripes (see Fig. 3). It is noted that this structure can mix with the zig-zag 2x1, producing a displacement in the zig-zag axis and/or a change of phase (see Fig. 4). This structure is slightly higher in energy than the zig-zag (Table 1) because it has a slightly reduced Al-Al average separation after the first nearest neighbor ring (Fig. 3). It appears at domain boundaries when misalignments occur (Fig. 4).

It is likely that the 2x1 zig-zag structure dominates basal plane Al_2O_3 ultrathin islands and films on refractory substrates, where the row orientation is determined by details of the nucleation process and surface defects. Note also that if a single additional row of either type exists in the 2x1 structure, as might be caused by a defect, the phase of the zig-zag is reversed across the anomaly. This may be seen by adding an additional *o*-row at the left edge of Fig. 2. If random islands grow into a film, there is only a 1/3 chance they will have the same row angular orientation. Even if two domains have the same angular orientation, there is only a 1/6 chance they will match (1/3 for alignment, see Fig. 4, and 1/2 for phase). Thus, because the zig-zag 1:1 pattern adds a linear aspect to the film symmetry, a loss of long range order easily occurs, causing an amorphous appearance to the Al sublattice in scattering experiments [12]. However, if considering barrier layers to corrosion, the film is still as dense as sapphire. Given a sufficiently defect-free Ru substrate, high annealing temperatures, and slow cooling, some 2x1 ordering may be observable.

Of all known aluminum oxide phases, the 2x1 zig-zag most closely resembles the so-called A plane of κ-Al_2O_3 [13]. This phase has -A-B-A-C- bulk stacking of close packed near-hexagonal O layers, and the A plane has an even mixture of *o* and *t*, arranged in alternating zig-zag rows (Fig. 2). The B and C planes have all *o*-ions [13]. This phase of alumina, stable at intermediary temperatures between γ- and the high temperature α-phase, is commonly produced by CVD and is used in the cut-

ting tool industry. Our results suggest it is the stability of the zig-zag 2x1 structure in the first Al_2O_3 layer that initially nucleates this phase during layer-by-layer growth.

We now turn to the subject of metal adhesion to the film. Recently, for the purpose of comparing differences, a survey of eleven adsorbed metals was made [17] using a model ultrathin Al_2O_3 film on Al(111), specifically the pure *t* structure (Fig. 1) [16]. In general, it was found that isolated metal adatoms are oxidized (i.e., are positive ions), donating their charge to the oxide itself, with most being taken up by neighboring oxygen atoms. All are strongly bound by several eV per atom. With transition metal adatoms from the left side of the periodic table, even multiply charged ions occur (this prediction was recently confirmed experimentally by the group of R. Madix [23]). In contrast, when three or more nearest neighbor metal interactions are present (i.e., at coverages of 2/3 ML or more) the ad-metal is metallic, with negligible or only minimal charge transfer to the oxide substrate. On a per atom basis, the resulting binding is then much weaker. Overall, these results closely resemble those for metals on sapphire(0001) [15].

For comparison to Refs. [15, 17], and to see if Al-sublattice structure and/or substrate stiffness affects adsorption, we present in Table 3 ad-metal LDA (and GGA) binding energies to the zig-zag 2x1 structure on Ru and on Al. Here, we assume commensurate 2 ML overlayers of Cu, Pd, and Pt, where the interface ad-metal atoms occupy atop-O sites, as has been shown to be universally preferred for metal thicknesses over 1ML [17]. It is seen that for the Al(111) substrate, *significant* increases in metal adhesion occur vs. the pure *t* film or the zig-zag film on Ru(0001), where energetics are also similar to bulk truncated sapphire [15]. In fact, for the Al(111) substrate, it is no longer true that isolated adatoms bind on a per atom basis much more strongly than do metallic overlayers!

Geometrically, there are several differences between the systems with the Al vs. Ru substrates: First, is the degree of vertical buckling in the layers (Table 2); and, second, is the degree of relaxation of Al ions at the oxide-surface (Table 2, right column). However, because the buckling of the oxygen ions at the film surface is similar between the two substrates, we conclude it is the second factor which is more causative to the large differences in binding. In fact, a closer examination of the film/substrate interface reveals a third difference, related to the second: During relaxation, additional Al

(now totalling four per unit cell) moves from the metal substrate vertically into the film (Table 2). These atoms are coordinated to and lie between both of the oxygen layers and have thus become ionic. *We propose it is this movement of substrate Al metal into the film which frees the Al ions at the film surface to rise and form lower energy interfaces with the overlying metals.* While the earlier study of film geometry [16] and metal binding at various coverages [17] found qualitatively similar adsorption as with sapphire(0001) [15], here we find differences of > 1 eV/atom (LDA) between the 1 ML Pt film on the 5 Å alumina film on Al(111) and Pt/sapphire(0001) [15].

A recent experimental study [24] used remarkable STM-determined nanocrystal Wulff shapes of Pd on Al_2O_3/NiAl(110) to derive a work of adhesion, W_{adh}, of 2.9 ± 0.2 J/m^2 between the Pd and the oxide film. This value is significantly greater than either the LDA (1.95 J/m^2) or GGA (1.05 J/m^2) values reported in Ref. [17], as discussed at some length [24]. We now explore the reasons for this disagreement.

One potential difference concerns the interatomic spacings in the Al_2O_3/NiAl(110) film, which has rotated film domains with respect to the substrate, and our computed films, where the O-O spacing at the film surface is the same as the interatomic spacing in the substrate metal. However, the recent analysis of TEM Moire patterns found a film lattice constant of 7.865 ± 0.065 Å [11], resulting in a film O-O spacing of 2.78 Å. This compares well with the 2.80 Å used here for the Al(111) substrate. Therefore, this slight strain does not produce an appreciable error or explain the disagreement.

Another possibility is the unrealistic oxide Al-sublattice structure used in Ref. [17]. However, here we report that this by itself did *not* cause a significant reduction in W_{adh} because the binding to the zig-zag film on the rigid Ru substrate resembles that to sapphire (0001) and to the model film (Fig. 1), where the high symmetry and small unit cell did though prevent the atom migrations described here for the zig-zag structure on Al(111), and the large adhesions seen in Table 3. Remarkably, however, the adhesion of Pd to the zig-zag film on Al(111) significantly *exceeds* that of 2.9 J/m^2 reported in Ref. [24] for the film on NiAl(110).

A final important difference is the rigidity of the NiAl(110) substrate compared with Al(111). This reduces the relaxations at the film/substrate interface, and increases the energy cost of extract-

ing Al from the substrate to permit the strong Al-ion motion towards the overlying Pd. To explore this aspect further, and test this conclusion, we have computed Pd GGA adhesion energies to zig-zag films on Al(111) where the Al substrate was frozen totally and except for the first layer. Indeed, as seen in Table 4, the increased rigidity has killed the increased adhesion, and causes the partially frozen result to approach that of the Ru substrate. In real systems, the ability to donate substrate metal atoms into the film is, of course, determined in turn by substrate stiffness and the related cohesive energy. Thus, with respect to metal adhesion, the film on NiAl(110) is quite *dis*similar to sapphire (and presumably to the other phases of pure alumina as well), and also dissimilar to a film of the same thickness on a more rigid substrate, Ru.

In summary, we have found that ultrathin alumina films most resemble the κ-phase of alumina, not the γ-phase. These results provide a natural explanation for observations that layer-by-layer CVD growth of alumina produces the κ-phase [13], that a loss of long range order can easily occur in the Al-sublattice [12], and are in agreement with earlier experiments concerning film surface termination [10] and the existence of a mixture of Al-ion types [10]. While Al-sublattice disorder can lead to these films being called amorphous, their density is still high, and the amorphous appearance does not necessarily lead to easier diffusion or greater susceptibility to chemical attack. However, movement of Al metal into the oxide layer has now been observed to be caused by ad-species, and thus the metal adsorption properties of ultrathin films depends critically on the nature of the underlying metal: Stiffer metals (e.g., Ru) cause a more sapphire-like response to adsorbates, while metals as soft as Al can increase adhesion even beyond that obtained by intermediate cases, as films on the Ni-Al materials [8, 9]. This causes us to conclude that the recently reported [24] adhesion strength of Pd to a film on NiAl(110) is a unique value, unlike that appropriate to pure alumina or to films on refractory metals such as Ru, and should not be expected to agree with theoretical numbers derived from studies of these systems.

Finally, note that the preferred interface between the overlying Pd metal and the relaxed oxide film on Al(111) did not have direct Pd-O contact, common for most metals deposited on alumina [17], and instead consisted of Pd-Al contact. This observation suggests that the basic structural rule

concerning metal/oxide interfaces may include a change as one moves far to the right in the periodic table, where the overlying metal may prefer cation rather than anion contact.

Acknowledgments

We thank R. Jürgen Behm and Flemming Besenbacher for sharing unpublished work, and Hans-Joachim Freund for valuable discussions. VASP was developed at the Institut für Theoretische Physik of the Technische Universität Wien. Sandia is a multiprogram laboratory operated by Sandia Corporation, a Lockheed Martin Company, for the United States Department of Energy under Contract DE-AC04-94AL85000. This work was partially supported by a Laboratory Directed Research and Development project.

References

[1] K. Wefers, Aluminum 37 (1961) 19; H. P. Godart, W. B. Jepson, M. R. Bothwell, and R. L. Kane, *Corrosion of Light Metals* (Wiley, New York, 1967); M. A. Barrett, *Studies with Ellipsometry* (Dept. of Metallurgy, The Norwegian Institute of Technology, 1967) p. III 4.

[2] J. Ahn and J. W. Rabalais, Surf. Sci., 388 (1997) 121.

[3] J. A. Kelber, C. Niu, K. Shepherd, D. R. Jennison and A. Bogicevic, Surf. Sci. 446 (2000) 76.

[4] G. Ertl and H.-J. Freund, Phys. Today, 52 (1999) 32, and references therein.

[5] J. M. DeTeresa, A. Barthelemy, A. Fert, J. P. Contour, F. Montalgne, and P. Seneor, Science 286 (1999) 507.

[6] A. Bogicevic and D. R. Jennison, Surf. Sci. 437 (1999) L741.

[7] N. Ernst, B. Duncombe, G. Bozdech, M. Naschitzki, and H.-J. Freund, Ultramicroscopy 79 (1999) 231.

[8] R. M. Jaeger, H. Kuhlenbeck, H.-J. Freund, M. Wuttig, W. Hoffmann, R. Franchy, H. Ibach, Surf. Sci., 259 (1991) 235.

[9] C. Becker, J. Kandler , H. Raaf, R. Linke, T. Pelster, M. Drager, M. Tanemura, K. Wandelt, J. Vac. Sci. Technol., A16 (1998) 1000.

[10] J. Libuda, F. Winkelmann, M. Baumer, H.-J. Freund, T. Bertrams, H. Neddermeyer, K. Muller, Surf. Sci., 318 (1994) 61.

[11] S. Nepijko, M. Klimenkov, H. Kuhlenbeck, R. Schlögl, and H.-J. Freund, Langmuir 15 (1999)

5309, and unpublished.

[12] F. B. de Mongeot, H. G. Keck, E. Kopatzki and R. J. Behm, Surf. Sci. (submitted).

[13] Y. Yourdshahyan, C. Ruberto, M. Halvarsson, L. Bengtsson, V. Langer, B. I. Lundqvist, S. Ruppi, U. Rolander, J. Amer. Ceramic Soc. 82 (1999) 1365; B. Holm, R. Ahuja, Y. Yourdshahyan, B. Johansson, B. I. Lundqvist, Phys. Rev. B. 59 (1999) 12777.

[14] C. Verdozzi, D. R. Jennison, P.A. Schultz, M. P. Sears, J. C. Barbour, and B. G. Potter, Phys. Rev. Lett., 80 (1998) 5615.

[15] C. Verdozzi, D. R. Jennison, P. A. Schultz, and M. P. Sears, Phys. Rev. Lett. 82 (1999) 799.

[16] D. R. Jennison, C. Verdozzi, P. A. Schultz, and M. P. Sears, Phys. Rev. B 59 (1999) R15605.

[17] A. Bogicevic and D. R. Jennison, Phys. Rev. Lett. 82 (1999) 4050.

[18] P. Hohenberg and W. Kohn, Phys. Rev. 136 (1964) B864; W. Kohn and L. J. Sham, Phys. Rev. 140 (1965) A1133; see also *Theory of the Inhomogeneous Electron Gas*, edited by S. Lundqvist and N. M. March (Plenum, New York, 1983).

[19] G. Kresse and J. Hafner, Phys. Rev. B 47 (1993) 558; 49 (1994) 14251; 54 (1996) 11169.

[20] D. Vanderbilt, Phys. Rev. B 32 (1985) 8412; 41 (1990) 7892.

[21] J. Perdew and A. Zunger, Phys. Rev. B **23** (1981) 5048; D. M. Ceperley and B. J. Alder, Phys. Rev. Lett. **45** (1980) 566.

[22] J. P. Perdew, J. A. Chevary, S. H. Vosko, K. A. Jackson, M. R. Pederson, D. J. Singh, and C. Fiolhais, Phys. Rev. B **46** (1992) 6671.

[23] R. J. Madix, J. Biener, M. Baumer, and A. Dinger, Faraday Diss. 114, see also the discussion section (in press).

[24] K. H. Hansen, T. Worren, S. Stempel, E. Laegsgaard, M. Baumer, H.-J. Freund, F. Besenbacher, and I. Stensgaard. Phys. Rev. Lett. 83 (1999) 4120.

Tables

Al sublattice:	octa-hedral	zig-zag 1:1 mix	stripe 1:1 mix	tetra-hedral
Ru(0001)	1.2	0.0	0.5	1.0
Al(111)	1.8	0.0	0.3	1.6

Table 1: Relative LDA energies in eV per Al_2O_3 unit of different stable flat Al_2O_3 films on Ru and Al substrates.

Atomic layer	Zig-Zag/Al(111)	Zig-Zag/Ru(0001)	2ML Pd/Zig-Zag/ Al(111)	2ML Pd/Zig-Zag/ Ru(0001)
Pd1	—	—	15.30, 15.34, 15.35	14.48, 14.50, 14.52
Pd2	—	—	13.09, 13.10, 13.14	12.15, 12.23, 12.28
O1	9.97, 10.07, 10.75	9.70, 9.82, 10.50	10.08, 10.20, 10.71	10.04, 10.11, 10.25
Al	9.94, 10.23	9.74, 9.79	**11.12, 11.13**	9.48, 9.58
O2	7.43, 8.08, 8.19	7.51, 7.74, 7.80	7.59, 7.84, 7.93	7.59, 7.80, 7.90
M1	6.80, 6.91, **8.31**	6.35, 6.44, 6.52	6.81, **8.38, 8.53**	6.36, 6.37, 6.46
M2	4.55, 4.57, 4.89	4.22, 4.24, 4.28	4.59, 4.60, 4.60	4.24, 4.25, 4.27

Table 2: LDA vertical positions in Å of all atoms for the clean zig-zag structure films on Al(111), Ru(0001), and the same films overlain by 2 ML of Pd. Symmetry causes different heights for each of three (two for the oxide Al layer) pairs of atoms within the 2x1 unit cell. M1 and M2 refer to the two first metallic substrate layers. Note the Al ions (shown in bold) when Pd is present have risen considerably *above* the O1 layer, made possible by Al atoms from the M1 row rising into the film.

Admetal:	Cu	Pd	Pt
strain:	+12%	4.4%	2.9%
zig-zag/Ru(0001)	1.2	0.8(0.6)	0.9
sapphire(0001)	0.5	1.0	0.5
pure *t*/Al(eV/atom)	0.9	0.8	0.5
zig-zag/Al (eV/atom)	1.5(1.2)	1.9(1.6)	2.0(1.7)
zig-zag/Al (J/m^2)	3.5(2.8)	4.5(3.8)	4.6(4.0)

Table 3: LDA(GGA, where available) adhesion energies in eV per interface metal atom of 2 ML of several metals to zig-zag Al_2O_3 films on Ru(0001) and Al(111). For comparison, LDA values on bulk truncated α-Al_2O_3(0001) [15] and on the pure *t*-model film [17] are also shown. The 2ML metal films prefer to align with the atop oxygen sites on the zig-zag oxide film surface. The lateral strain is also shown, as are the adhesion energies (on the film with the Al-substrate) in J/m^2, for comparison to Ref. [24].

Substrate freedom:	All frozen	Only top layer free	All free
zig-zag/Al(111) (eV/atom)	0.4	0.5	1.6

Table 4: GGA adhesion energy in eV per interface metal atom of 2ML of Pd to zig-zag films where the slab substrate of Al(111) is frozen in various degrees at the LDA relaxed positions of the bulk metal.

Figure Captions

Fig. 1: The 5 Å (two O-layer) pure *t* film on Al(111), which shows the chemisorbed nature of the first O-layer and the coplanarity of the surface Al_2O_3 layer (from Ref. [16]).

Fig. 2: Top view of the 2x1 zig-zag structure with even numbers of *t* (red) and *o* (blue) Al-ions (right side) compared with the pure tetrahedral structure (left side). Also shown are the unit cells, and the differences in nearest neighbor Al-Al distances. The central arrows show how a *t*-row may be displaced to create the 2x1 structure while preserving coordination.

Fig. 3: The striped structure (bottom), also an even mixture of *t* and *o*, compared with the zig-zag structure (top). Also shown are the differences in the nearest neighbor shell which causes the stripe structure to be higher in energy.

Fig. 4: Examples of domain boundaries of the 2x1 zig-zag structure which can occur when the overall direction of the rows are aligned. The lines indicate where phase changes and displacements occur.

Two O-layer Al_2O_3 film on Al(111)

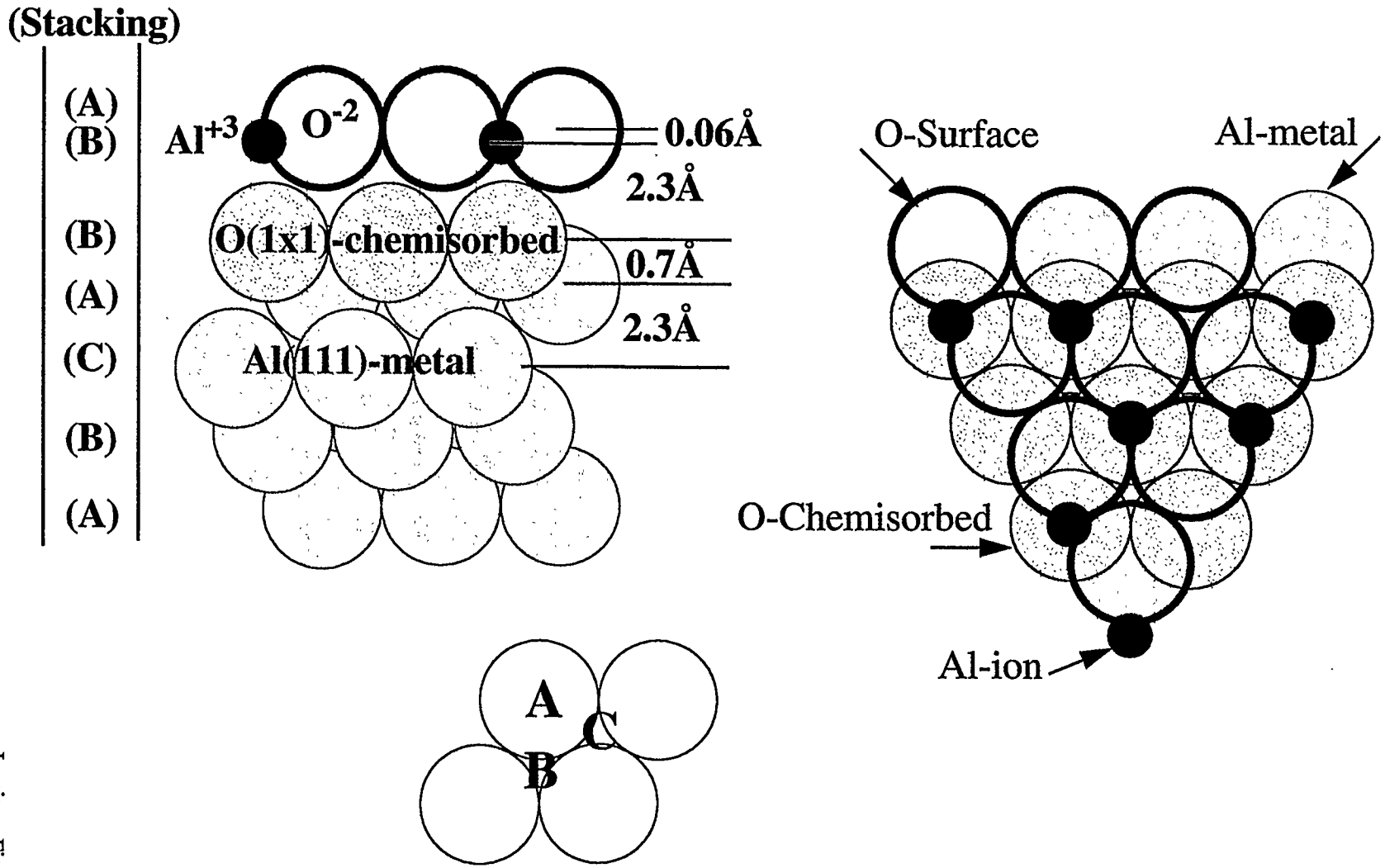

Jennison, Figure 1.

Pure Tetrahedral (left) going to Zig-Zag (right).

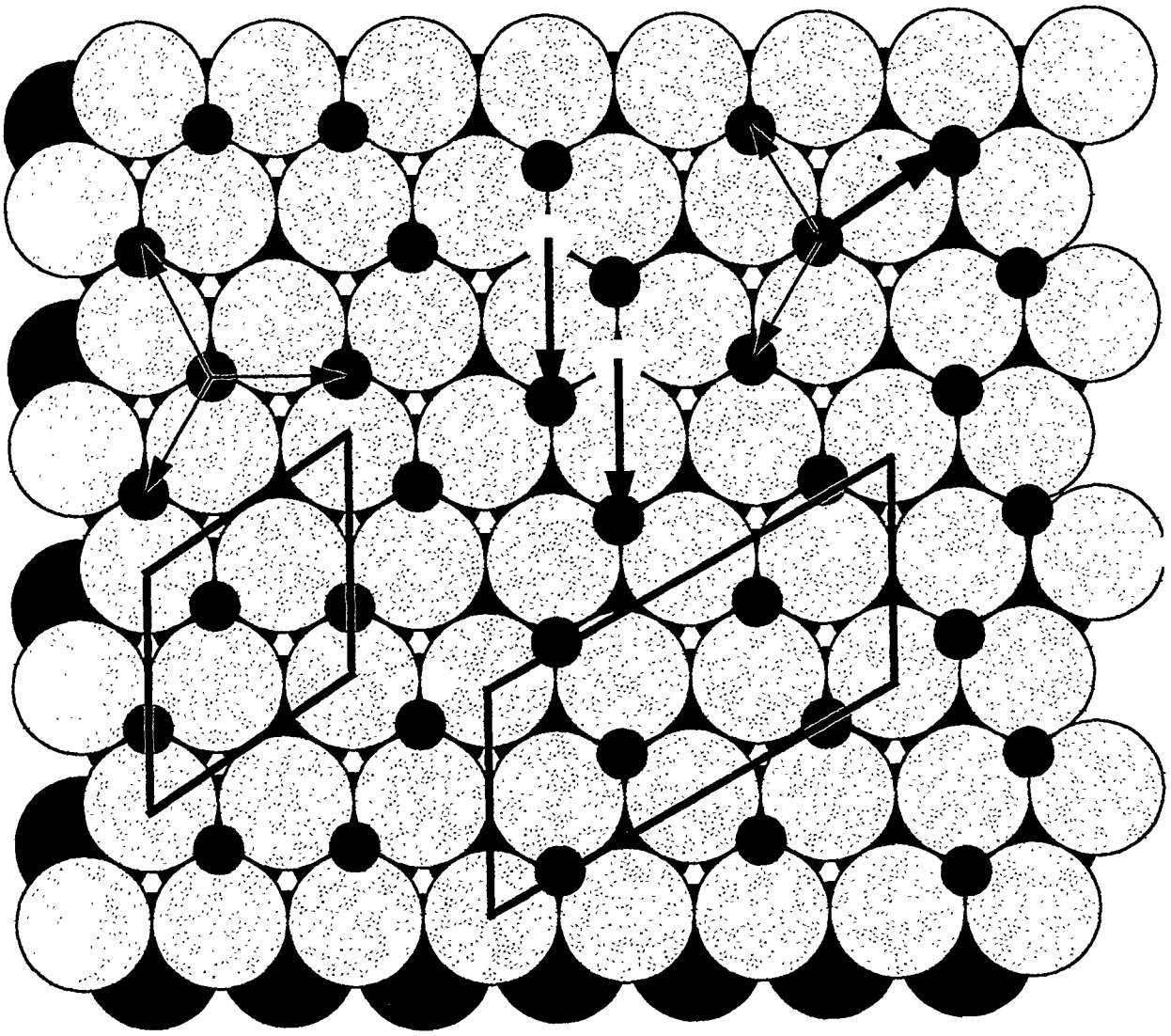

Jennison, Figure 2

Zig-Zag (top) going to Stripe (bottom).

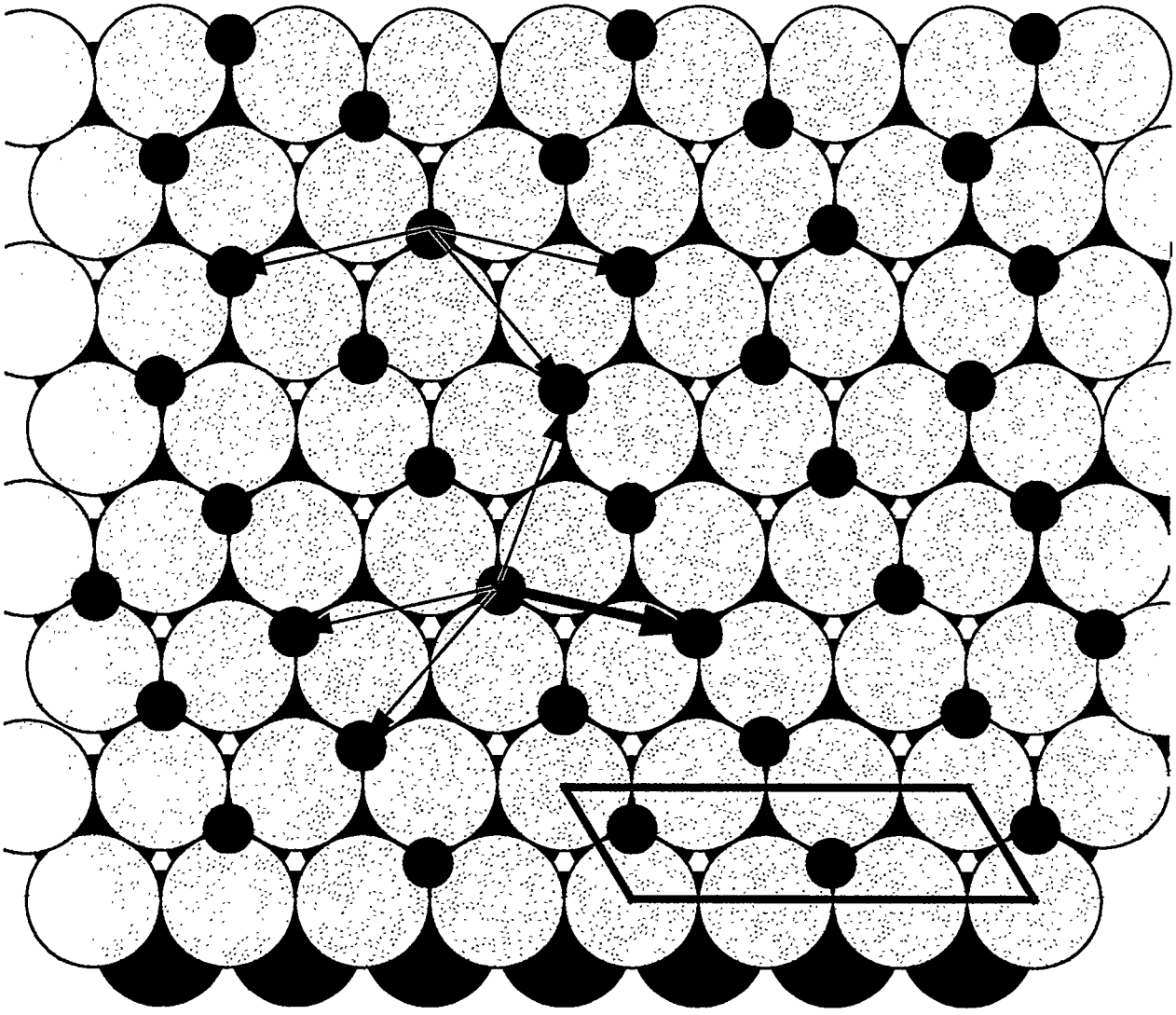

Jennison, Figure 3

Example: Domain Boundaries When Angularly Aligned.

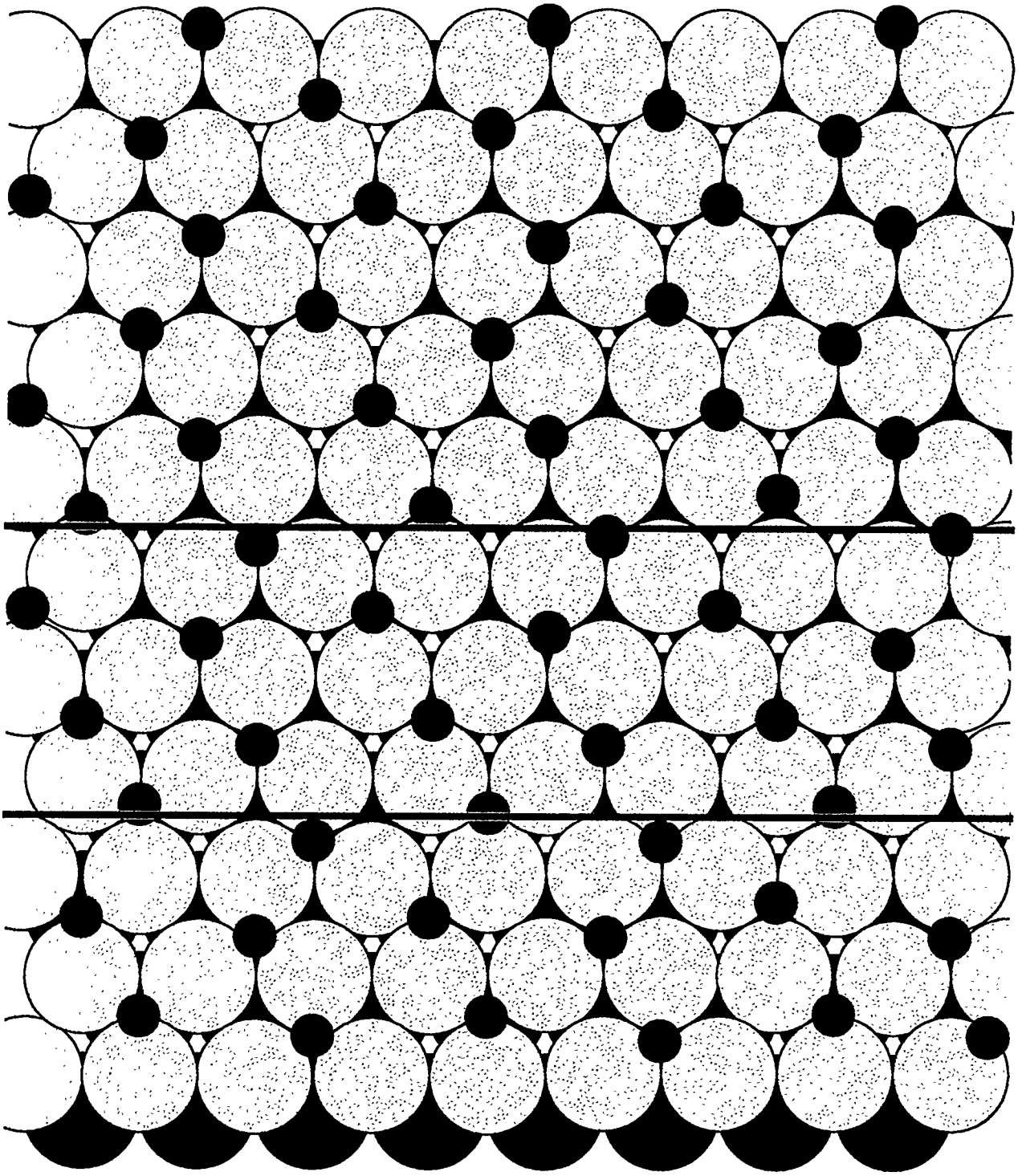

Jennison, Figure 4